N$_2$ Binding to an Iron-Sulfur-Carbon Site

Ilija   ori [1], **Brandon Q. Mercado**[1], **Eckhard Bill**[2], **David J. Vinyard**[1], and **Patrick L. Holland**[1]

[1]Department of Chemistry, Yale University, 225 Prospect Street, New Haven, Connecticut 06520, USA

[2]Max Planck Institute for Chemical Energy Conversion, Stiftstrasse 34-36, D-45470 Mülheim an der Ruhr, Germany

Abstract

Nitrogenases are found in some microorganisms, and these enzymes convert atmospheric N$_2$ to ammonia, thereby providing essential nitrogen atoms for higher organisms. Some nitrogenases reduce atmospheric N$_2$ at the FeMoco, a sulfur-rich iron-molybdenum cluster[1–5]. The iron centers that are coordinated to sulfur and carbon atoms in FeMoco have been proposed as the substrate binding sites, based on kinetic and spectroscopic studies[5,6]. Studies on the enzyme indicate that iron atom Fe6 and possibly also adjacent belt iron sites are involved.[5–8] In the resting state, the central Fe sites (including Fe6) have identical environments consisting of three sulfides and a carbide. Addition of electrons to the resting state causes the FeMoco to react with N$_2$, but the geometry and bonding environment of N$_2$-bound species remain unknown[5]. In this manuscript, we describe a synthetic complex with a sulfur-rich coordination sphere that, upon reduction, breaks an Fe-S bond and binds N$_2$. The product is the first synthetic Fe–N$_2$ complex in which iron has bonds to sulfur and carbon atoms, providing a model for N$_2$ coordination in the FeMoco. Our results demonstrate that breaking an Fe-S bond is a chemically reasonable route to N$_2$ binding in the FeMoco, and show structural and spectroscopic details for weakened N$_2$ on a sulfur-rich iron site.

N$_2$ binding to FeMoco is believed to take place at an iron center with three sulfur ligands following Fe-C bond elongation or dissociation (I to II, Fig. 1A)[9–15]. These sites could accommodate N$_2$ binding by breaking an Fe-S or an Fe-C bond, but data on the enzyme do not yet distinguish between these possibilities. The likely enzymatic intermediates, iron-N$_2$ species supported either solely by sulfur, or by sulfur and carbon ligands, are unprecedented in isolated coordination complexes. Here, we focus on an alternative hypothesis where one of the Fe-S bonds at the active site is broken upon reduction/protonation to expose the N$_2$

binding site (**I** to **III**, Fig. 1A)[16,17]. N_2 would thus bind at a pseudotetrahedral S,S,C-bound iron site. The feasibility of Fe-S bond cleavage in FeMoco is experimentally supported by the loss of this S atom in the structure of CO-inhibited nitrogenase[7], and by the observation of Fe-S cleavage upon protonation in smaller FeS clusters[18,19]. Other N_2 binding hypotheses include side-on binding, bridging, and *endo* coordination where N_2 is positioned close to three additional iron atoms and opposite to a sulfur atom (**IV**, Fig. 1A)[5,11,17].

Iron-N_2 complexes supported solely by sulfur, or by sulfur and carbon supporting ligands, are likely N_2-bound species in the nitrogenase catalytic cycle, but they are experimentally unprecedented. Though chemists have prepared complex iron-sulfur clusters inspired by the multimetallic structure of FeMoco, N_2 does not bind to any known synthetic iron-sulfur cluster[20]. A number of well-defined iron complexes with B, N, and P supporting ligands are known to activate N_2, and Peters has established P- and C-based systems capable of performing catalytic reduction of N_2 to ammonia[14,15,21–24]. A few iron-N_2 complexes have thioether/thiolate donors on the same iron center, and each is additionally supported by P- or N- donors[25–27]. To the best of our knowledge, there are no examples of terminal N_2 complexes of any metal having immediate ligand environments similar to those in **II-IV**, which hinders scientists' ability to predict the behavior of the FeMoco.

For this work, we designed bis(thiolate) ligand **L²⁻**, which offers only sulfur and carbon based coordination sites (indicated by yellow and grey spheres in Fig. 1B). Our approach was guided by the proposed binding mode **III** in Fig. 1A, which requires the presence of two coordinating sulfur atoms. These are provided by two chelating arylthiolate donors with bulky 2,4,6-triisopropylphenyl groups shielding the S sites. A central aromatic ring connects the two arylthiolate arms and additionally provides potential carbon based attachment sites[28]. Although carbide is electronically different than the arene ring in **L²⁻**, each could provide flexible bonding for stabilization of various intermediates during ammonia production[14,15].

Iron(II) ions were installed in the ligand framework by treating **LH₂** with iron(II) bis(bis(trimethylsilyl)amide) in tetrahydrofuran (THF), which yielded the bright yellow, high spin iron(II) complex LFe(THF)₂ (**1**, Fig. 2A). Its crystal structure reveals that it is four-coordinate, and that all Fe-C distances are at least 2.59 Å (Fig. 2B). Reduction of **1** to iron(I) with potassium graphite (KC₈) results in the formation of brown-yellow **2**, with close Fe-C distances (2.04 – 2.12 Å) indicating η^6-binding of the central arene ring (Fig. 2A, 2C). Comparison of the molecular structures of **1** and **2** reveals that rotation of the arylthiolate arms enables the central aryl ring to move closer to the iron atom. Compound **2** has a rhombic EPR (electron paramagnetic resonance) spectrum with **g** = [2.180, 2.020, 1.989] and a solution magnetic moment of 2.1 μ_B, which indicate a low-spin ($S = 1/2$) iron(I) center.

Encouraged by the ability of the ligand to stabilize low-valent iron sites, we further reduced the iron site to the iron(0) oxidation state. Reduction of a brown-yellow solution of **2** with one equivalent of KC₈ under one atmosphere of N_2 at −70 °C resulted in an immediate color change to deep red. After addition of 18-crown-6 to sequester potassium cations, dark red-brown crystals of **3** grew at −40 °C. X-ray diffraction analysis shows that **3** is [LFeN₂]

[K(18-crown-6)(THF)$_2$]$_2$ (Fig. 2A and 3A). In **3**, N$_2$ is bound as a terminal ligand at a pseudotetrahedral iron(0) site, which is further bound to two S atoms and the arene of the supporting ligand. The closest Fe-C distance in **3** is 2.04 Å, and there is a second carbon atom within bonding distance (Fe-C = 2.24 Å), indicating asymmetric η^2 coordination of the arene. The potassium cations do not bind to the N$_2$ ligand.

The new N$_2$ complex **3** provides a structural model of the pseudotetrahedral S,S,C supported N$_2$ binding mode **III** proposed for FeMoco (Fig. 1A). It is compared to the experimental structures of resting state FeMoco and CO-inhibited FeMoco in Fig. 3B[2,7]. In the fourth coordination site that has labile S and CO ligands in nitrogenase structures[7], **3** contains an N$_2$ ligand. The Fe-S bond distances in **3** (2.32–2.35 Å) are somewhat longer than the Fe-S bonds in resting state FeMoco (2.25–2.27 Å), due to either the lesser negative charge of the thiolate or the greater steric hindrance. Remarkably, the Fe-C distance in **3** at 2.04 Å is very close to the Fe6-carbide distance of 2.01 Å in FeMoco structures. Overall, the relatively simple ligand **L**$^{2-}$ is capable of arranging appropriate atoms around iron and imparting a geometry that resembles the likely active iron site in FeMoco structures. However, the electronic structure of the iron(0) complex **3** may be different than the iron site in the N$_2$-binding form of the FeMoco (for which the structure and iron oxidation state are unknown).

Next, we designed a compound (**5**) intended to test the idea that Fe-S bond dissociation could provide a coordination site for N$_2$ binding (**I** to **III** in Fig. 1A). The bis(thiolate) complex **1** reacted with thiolate **4** to give the iron tris(thiolate) complex **5** (Fig. 2A). This orange high-spin iron(II) complex contains three S ligands, like Fe6 in the FeMoco resting state (**I** in Fig. 1). The interaction of iron with the central arene ring is weak, with the closest Fe-C distance at 2.48 Å (Fig. 2D). Thus we view this site as three-coordinate and unsaturated, which is supported by the reversible binding of one THF molecule at low temperature (Fig. 2E and Supplementary Information show the X-ray crystal structure of **5**·THF and temperature-dependent UV-vis spectra).

The tris(thiolate) iron(II) site in **5**/**5**·THF was reduced to the iron(0) oxidation level with just over two equivalents of KC$_8$, under conditions otherwise equivalent to those used for reduction of the iron(I) bis(thiolate) complex **2** (Fig. 2A). This yielded the same N$_2$ complex **3** described above, and 1.0 equiv. of free thiolate was produced. Reduction thus causes an Fe-S bond to break concomitant with N$_2$ binding, as in the proposed pathway for N$_2$ binding to FeMoco in Fig. 1A (**I** to **III**). We note that tris(thiolate) **5** contains all the nearby atoms to support alternative binding modes **II** and **IV** in Fig. 1A, but Fe-S dissociation takes place instead.

We return to describe the further characterization of **3**, which gives insight into potential properties of N$_2$ after binding at FeMoco. Though complex **3** is very thermally sensitive, it was possible to isolate pure samples of **3** in >80% yield from reduction of **5** at low temperature and washing the crystals with cold butane at −70 °C. Analysis of these crystals by Mössbauer spectroscopy confirms the presence of a single iron species. Infrared spectroscopy (IR) analysis of single crystals of **3** revealed a strong N-N stretching band at 1880 cm^{-1}. These frequencies are the lowest observed for any Fe-N$_2$ complex with a terminal N$_2$ ligand[23], which shows that the thiolates are powerful electron donors that enable

substantial backbonding into the N_2 π* orbitals. The N_2 ligand in **3** exchanges with free $^{15}N_2$ (giving an ^{15}N-^{15}N stretching band at 1813 cm^{-1}) at −70 °C in the solid state. Samples of **3** kept at room temperature for a few hours lack the N_2 stretching vibration, further demonstrating the lability of N_2. The lability suggests that the Fe-N_2 interaction, though strong as judged by IR spectroscopy, may be compensated with tighter binding to the arene ring.

Compound **3** has a high spin ($S = 1$) electronic configuration, as determined by SQUID (superconducting quantum interference device) magnetometry on a crystalline sample. This experimental observation was confirmed with density functional theory calculations on a truncated model of **3**. Optimization with $S = 1$ gave a model close to the experimental geometry, but optimization with $S = 0$ gave significantly different bond lengths and angles, and a Gibbs free energy (G°) that was higher by 37 kJ/mol (see Supplementary Information). High spin iron(0) dinitrogen complexes are rare, and have been seen mainly in cases where high symmetry makes the frontier orbitals nearly degenerate[29,30]. To our knowledge, **3** is the first high spin iron complex that contains both S and N_2 ligands[25,26], and shows that high-spin iron (as expected in the weak-field sulfur-dominated environment of iron atoms in the FeMoco) can activate N_2 substantially.

The preparation of an iron-N_2 complex with a sulfur-rich environment provides structural and spectroscopic precedents for FeMoco-N_2 binding, and also gives insight into the nitrogenase mechanism. Reduction of complex **5** breaks an Fe-S bond as in the hypothetical conversion of **I** to **III** in the FeMoco (Fig. 1), and binds N_2 in a form where the N-N bond is greatly weakened. In this way, the results support the idea that the sulfur-rich iron site in the FeMoco is particularly well-suited for N_2 activation, and that Fe-S bonds can be easily broken upon reduction to allow binding of N_2.

Supplementary Material

Refer to Web version on PubMed Central for supplementary material.

Acknowledgments

References

1. Einsle O, et al. Nitrogenase MoFe-Protein at 1.16 Å Resolution: A Central Ligand in the FeMo-Cofactor. Science. 2002; 297:1696–1700. [PubMed: 12215645]

2. Spatzal T, et al. Evidence for Interstitial Carbon in Nitrogenase FeMo Cofactor. Science. 2011; 334:940. [PubMed: 22096190]

3. Lancaster KM, et al. X-ray Emission Spectroscopy Evidences a Central Carbon in the Nitrogenase Iron-Molybdenum Cofactor. Science. 2011; 334:974–977. [PubMed: 22096198]

4. Wiig JA, Hu Y, Lee CC, Ribbe MW. Radical SAM-Dependent Carbon Insertion into the Nitrogenase M-Cluster. Science. 2012; 337:1672–1675. [PubMed: 23019652]

5. Hoffman BM, Lukoyanov D, Yang ZY, Dean DR, Seefeldt LC. Mechanism of Nitrogen Fixation by Nitrogenase: The Next Stage. Chem Rev. 2014; 114:4041–4062. [PubMed: 24467365]

6. Seefeldt LC, Hoffman BM, Dean DR. Mechanism of Mo-Dependent Nitrogenase. Annu Rev Biochem. 2009; 78:701–722. [PubMed: 19489731]

7. Spatzal T, Perez KA, Einsle O, Howard JB, Rees DC. Ligand binding to the FeMo-cofactor: Structures of CO-bound and reactivated nitrogenase. Science. 2014; 345:1620–1623. [PubMed: 25258081]

8. Yandulov DV, Schrock RR. Catalytic Reduction of Dinitrogen to Ammonia at a Single Molybdenum Center. Science. 2003; 301:76–78. [PubMed: 12843387]

9. Holland PL. Low-coordinate iron complexes as synthetic models of nitrogenase. Can J Chem. 2005; 83:296–301.

10. MacBeth CE, Harkins SB, Peters JC. Synthesis and characterization of cationic iron complexes supported by the neutral ligands $NP^{i\text{-}Pr}_3$, $NArP^{i\text{-}Pr}_3$, and $NS^{t\text{-}Bu}_3$. Can J Chem. 2005; 83:332–340.

11. Dance I. Ramifications of C-centering rather than N-centering of the active site FeMo-co of the enzyme nitrogenase. Dalton Trans. 2012; 41:4859–4865. [PubMed: 22395244]

12. Hinnemann B, Nørskov JK. Chemical Activity of the Nitrogenase FeMo Cofactor with a Central Nitrogen Ligand: Density Functional Study. J Am Chem Soc. 2004; 126:3920–3927. [PubMed: 15038746]

13. George SJ, et al. EXAFS and NRVS Reveal a Conformational Distortion of the FeMo-cofactor in the MoFe Nitrogenase Propargyl Alcohol Complex. J Inorg Biochem. 2012; 112:85–92. [PubMed: 22564272]

14. Creutz SE, Peters JC. Catalytic Reduction of N_2 to NH_3 by an Fe–N_2 Complex Featuring a C-Atom Anchor. J Am Chem Soc. 2014; 136:1105–1115. [PubMed: 24350667]

15. Anderson JS, Rittle J, Peters JC. Catalytic conversion of nitrogen to ammonia by an iron model complex. Nature. 2013; 501:84–87. [PubMed: 24005414]

16. Kästner J, Blöchl PE. Ammonia Production at the FeMo Cofactor of Nitrogenase: Results from Density Functional Theory. J Am Chem Soc. 2007; 129:2998–3006. [PubMed: 17309262]

17. Schimpl J, Petrilli HM, Blöchl PE. Nitrogen Binding to the FeMo-Cofactor of Nitrogenase. J Am Chem Soc. 2003; 125:15772–15778. [PubMed: 14677967]

18. Alwaaly A, Dance I, Henderson RA. Unexpected explanation for the enigmatic acid-catalysed reactivity of $[Fe_4S_4X_4]^{2-}$ clusters. Chem Commun. 2014; 50:4799–4802.

19. Saouma CT, Morris WD, Darcy JW, Mayer JM. Protonation and Proton-Coupled Electron Transfer at S-Ligated [4Fe-4S] Clusters. Chem Eur J. 2015; 21:9256–9260. [PubMed: 25965413]

20. Lee SC, Lo W, Holm RH. Developments in the Biomimetic Chemistry of Cubane-Type and Higher Nuclearity Iron–Sulfur Clusters. Chem Rev. 2014; 114:3579–3600. [PubMed: 24410527]

21. Ung G, Peters JC. Low-Temperature N_2 Binding to Two-Coordinate L_2Fe^0 Enables Reductive Trapping of $L_2FeN_2^-$ and NH_3 Generation. Angew Chem Int Ed. 2015; 54:532–535.

22. Rodriguez MM, Bill E, Brennessel WW, Holland PL. N_2 Reduction and Hydrogenation to Ammonia by a Molecular Iron-Potassium Complex. Science. 2011; 334:780–783. [PubMed: 22076372]

23. Hazari N. Homogeneous iron complexes for the conversion of dinitrogen into ammonia and hydrazine. Chem Soc Rev. 2010; 39:4044–4056. [PubMed: 20571678]

24. Danopoulos AA, Wright JA, Motherwell WB. Molecular N_2 complexes of iron stabilised by *N*-heterocyclic 'pincer' dicarbene ligands. Chem Commun. 2005:784–786.

25. Takaoka A, Mankad NP, Peters JC. Dinitrogen Complexes of Sulfur-Ligated Iron. J Am Chem Soc. 2011; 133:8440–8443. [PubMed: 21574618]

26. Bart SC, Lobkovsky E, Bill E, Wieghardt K, Chirik PJ. Neutral-Ligand Complexes of Bis(imino)pyridine Iron: Synthesis, Structure, and Spectroscopy. Inorg Chem. 2007; 46:7055–7063. [PubMed: 17655227]

27. Creutz SE, Peters JC. Diiron Bridged-Thiolate Complexes That Bind N_2 at the $Fe^{II}Fe^{II}$, $Fe^{II}Fe^{I}$, and $Fe^{I}Fe^{I}$ Redox States. J Am Chem Soc. 2015; 137:7310–7313. [PubMed: 26039253]

28. Ellison JJ, Ruhlandt-Senge K, Power PP. Synthesis and Characterization of Thiolato Complexes with Two-Coordinate Iron(II). Angew Chem Int Ed Engl. 1994; 33:1178–1180.

29. Suess DLM, Peters JC. H–H and Si–H Bond Addition to Fe≡NNR_2 Intermediates Derived from N_2. J Am Chem Soc. 2013; 135:4938–4941. [PubMed: 23472709]

30. Moret ME, Peters JC. Terminal Iron Dinitrogen and Iron Imide Complexes Supported by a Tris(phosphino)borane Ligand. Angew Chem Int Ed. 2011; 50:2063–2067.
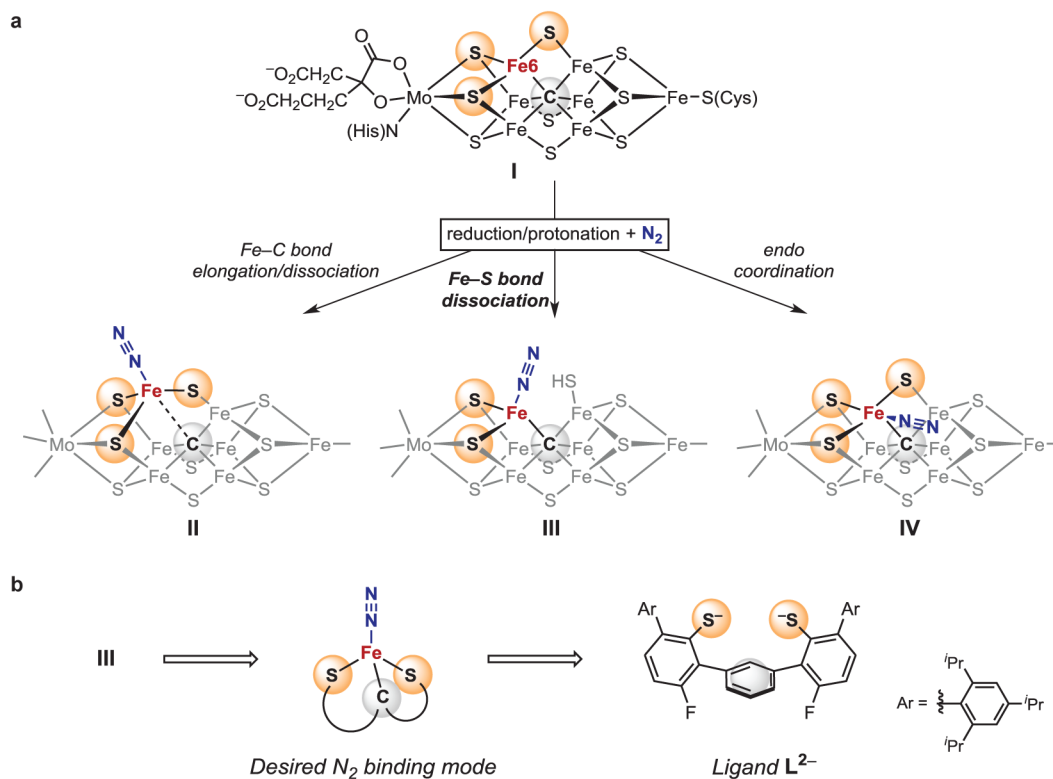
Figure 1. N$_2$ binding to iron in sulfur and carbon rich environments
a, Schematic representations of FeMoco and three potential N$_2$ binding modes. Potentially protonated sulfur ligands are not specified. **b**, Ligand design for a synthetic sulfur-carbon site.
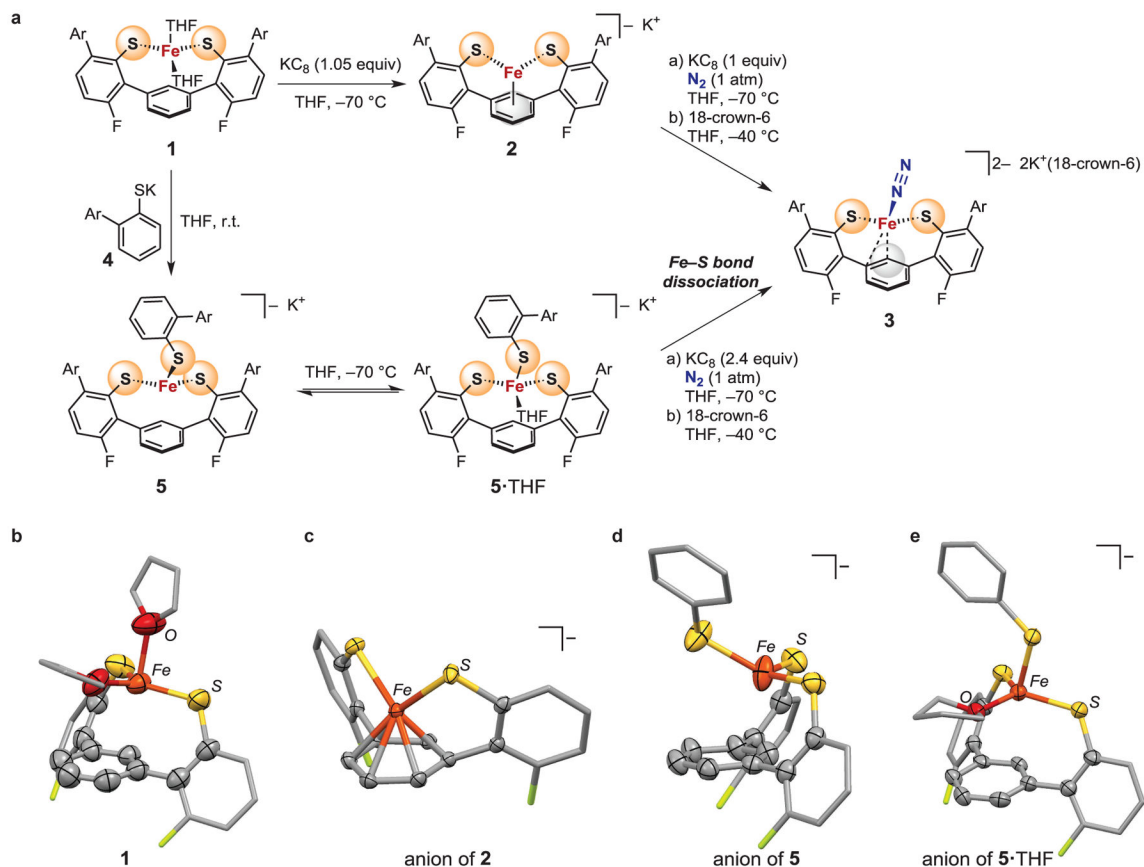
Figure 2. N$_2$ binding at an iron-sulfur-carbon site through Fe-S bond cleavage

a, Reactions of synthetic iron-sulfur sites leading to N$_2$-binding. The bottom pathway shows Fe-S cleavage with N$_2$ binding. Ar = 2,4,6-triisopropylphenyl. **b–e**, Molecular structures of the synthetic mononuclear iron-sulfur sites presented here. Hydrogen atoms and Ar groups are omitted for clarity.
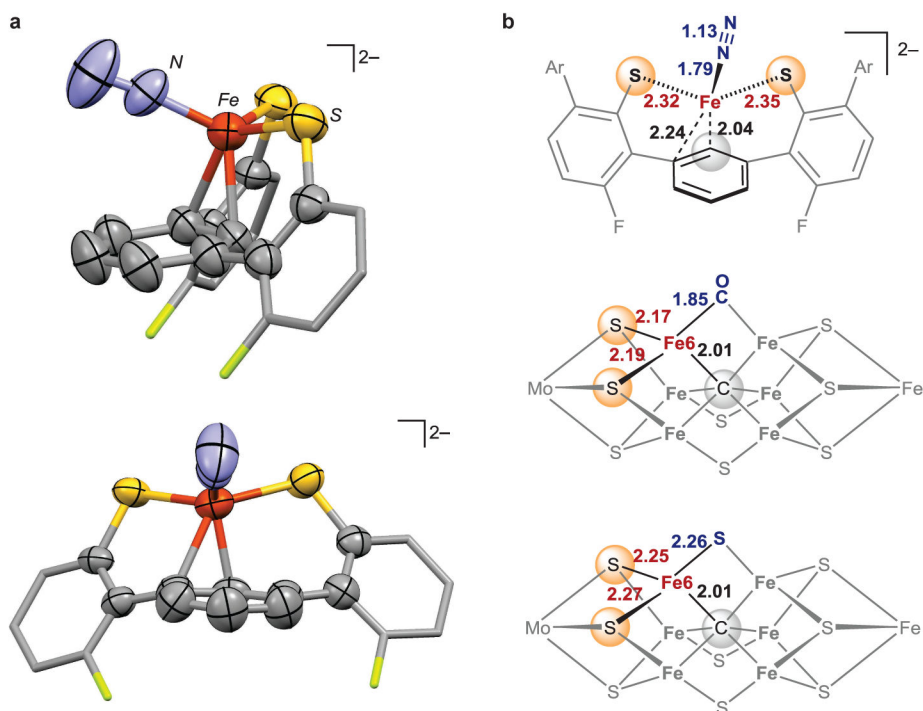
Figure 3. Iron-N₂ complex supported by sulfur and carbon ligands
a, Two views of the molecular structure of the anionic part of **3**. Hydrogen atoms and Ar groups are omitted. **b**, Comparison of geometric parameters with CO-inhibited FeMoco[7] and resting state FeMoco[2]. All distances are reported in Ångstrøms.